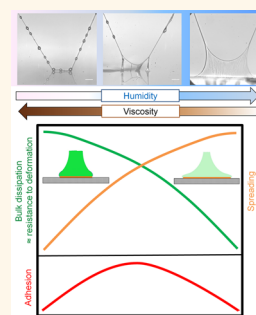


# Spiders Tune Glue Viscosity to Maximize Adhesion

Gaurav Amarpuri,<sup>†</sup> Ci Zhang,<sup>†</sup> Candido Diaz,<sup>‡</sup> Brent D. Opell,<sup>§</sup> Todd A. Blackledge,<sup>‡</sup> and Ali Dhinojwala<sup>\*,†</sup>

<sup>†</sup>Department of Polymer Science and <sup>‡</sup>Department of Biology, Integrated Bioscience Program, The University of Akron, Akron, Ohio 44325, United States and <sup>§</sup>Department of Biological Sciences, Virginia Tech, Blacksburg, Virginia 24061, United States

**ABSTRACT** Adhesion in humid conditions is a fundamental challenge to both natural and synthetic adhesives. Yet, glue from most spider species becomes stickier as humidity increases. We find the adhesion of spider glue, from five diverse spider species, maximizes at very different humidities that matches their foraging habitats. By using high-speed imaging and spreading power law, we find that the glue viscosity varies over 5 orders of magnitude with humidity for each species, yet the viscosity at maximal adhesion for each species is nearly identical,  $10^5$ – $10^6$  cP. Many natural systems take advantage of viscosity to improve functional response, but spider glue's humidity responsiveness is a novel adaptation that makes the glue stickiest in each species' preferred habitat. This tuning is achieved by a combination of proteins and hygroscopic organic salts that determines water uptake in the glue. We therefore anticipate that manipulation of polymer–salts interaction to control viscosity can provide a simple mechanism to design humidity responsive smart adhesives.



**KEYWORDS:** humidity · adhesion · viscosity · spider silk · orb web · viscid glue · aggregate protein

Humidity plays a pervasive role in shaping the properties of biological materials. Burying of seeds by wheat-awns,<sup>1</sup> optimal orientation of branches in spruce trees,<sup>2</sup> and pollen adhesion<sup>3</sup> are all actuated by water uptake in response to changes in relative humidity (RH, %) of air. However, high humidity usually hinders adhesion, as seen in most synthetic adhesives.<sup>4,5</sup> In contrast, spider viscid glue becomes stickier as humidity increases,<sup>6–9</sup> more than doubling adhesion at humidities as high as 90% RH in some spider species.<sup>8</sup> The impressive diversity of orb-weaving spiders (~5500 species)<sup>10</sup> attests to how effectively silk glues adhere to insects, making it important to understand how humidity impacts glue performance. The habitats of these species vary from extremely arid to very moist environments, suggesting that how viscid glue responds to humidity may facilitate adaptation to the local environment. Increase in interfacial water at high humidity decreases adhesion of synthetic glues,<sup>4,5</sup> and understanding how spiders overcome this limitation can help in designing better adhesives for humid environments.

The viscid silk in orb-weaving spiders consists of a pair of central flagelliform silk threads with evenly spaced glue droplets produced by the aggregate glands.<sup>11,12</sup>

These glue droplets, which self-organize due to capillary forces,<sup>13,14</sup> consist of glycoproteins<sup>15,16</sup> in a mixture of water and low molecular weight inorganic and organic salts.<sup>15,17–19</sup> These salts are hygroscopic and constitute 40–60% of the total weight of the web.<sup>13,17,18</sup> The salts play an important role in keeping the glue moist and stabilizing the glycoproteins.<sup>20</sup> Also, the salts and glycoproteins are intermixed with each other,<sup>19</sup> rather than phase-separated as an earlier model proposed.<sup>13,21</sup> With increase in humidity, the glue droplet can swell and almost double its size<sup>6–9</sup> reducing glue viscosity. Viscoelastic adhesion theory<sup>22</sup> predicts that glue adhesion is controlled by two dominating factors: interfacial adhesion and bulk dissipation. At low humidity, the glue is solid and cohesively strong, but it is unable to spread and thus has low interfacial adhesion. At high humidity, glue sequesters water from atmosphere, thereby increasing in size and spreading over a larger area (high interfacial adhesion) but resulting in low bulk dissipation (more liquid-like). Thus, we anticipate an optimum humidity where adhesion is maximum.<sup>6</sup>

We hypothesize that natural selection has tuned the glue viscosity to maximize adhesion to match the foraging humidity of spiders. To test this hypothesis, we have

\* Address correspondence to ali4@uakron.edu.

Received for review September 8, 2015 and accepted October 29, 2015.

Published online October 29, 2015  
10.1021/acs.nano.5b05658

© 2015 American Chemical Society

TABLE 1. Spider Species and Their Habitats

species	foraging conditions	
	time	microhabitat
<i>Argiope trifasciata</i>	diurnal	open field <sup>23</sup>
<i>Larinioides cornutus</i>	nocturnal	near water-bodies <sup>24,25</sup>
<i>Verrucosa arenata</i>	diurnal	edge of forests <sup>25</sup>
<i>Neoscona crucifera</i>	nocturnal	forest <sup>26</sup>
<i>Tetragnatha laboriosa</i>	nocturnal	above water <sup>25</sup>

selected five spider species that are active in very different microhabitats (Table 1). We demonstrate an intriguing correlation between maximum adhesion and optimum range of viscosity for all five spider species. This suggests a very simple and elegant approach of tuning adhesion by controlling water uptake through the use of hygroscopic salts.

## RESULTS

**Adhesion Testing.** Figure 1 shows the normalized work done during peeling of capture threads for the five spider species at four different humidities, 30, 50, 70, and 90% RH. The data are normalized to the lowest value within each species because the absolute peeling work depends on the size and spacing of the glue droplets, both of which differ across species. The absolute value of peeling work is reported in Table S1. The contact time of thread with the substrate and the peeling rate were kept constant in all the measurements (see Experimental Section).

The peeling work is responsive to environmental humidity for all species. Interestingly, maximum adhesion occurs at the humidity closest to the foraging humidity of each species. For example, *Argiope* viscid thread shows maximum adhesion at RH of 30–50% and declines significantly at higher humidity. This correlates well with *Argiope* ecology because they are active during the day in the fields, where the humidity averages 40–50% RH.<sup>9</sup> On the other extreme, the adhesion of *Tetragnatha* viscid thread continues to increase close to 100% RH. This again matches well with *Tetragnatha* ecology because they build webs at night in extremely moist environments just above the streams.<sup>25</sup> Similarly, *Verrucosa*, *Larinioides*, and *Neoscona* all showed maximum adhesion at intermediate humidity, which is close to the humidity at which they forage.<sup>8,25</sup>

The work done during peeling spider viscid silk includes contributions from two components: glycoprotein glue and the flagelliform fiber that supports the glue droplets (Figure 2B). Using the model developed by Sahni et al.,<sup>27</sup> we decoupled the work done by the glue and the fibers. Both components contribute similarly to the total peeling work (Supporting Information, Section 2 (SI-2)), suggesting that both the flagelliform fibers and the glue have an optimum

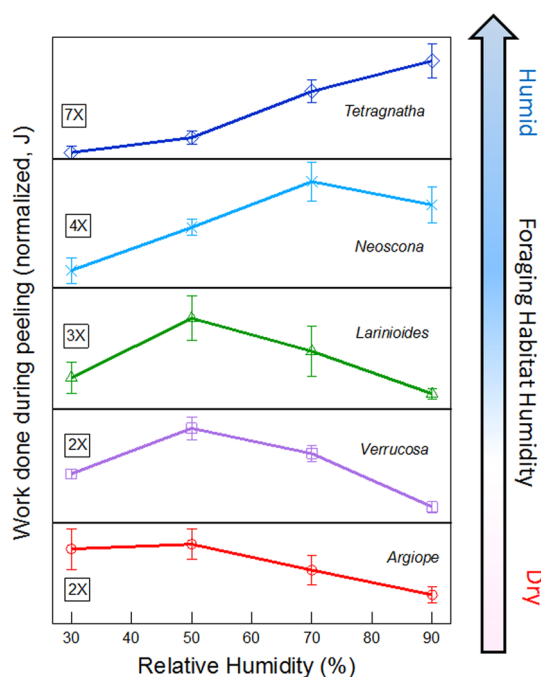
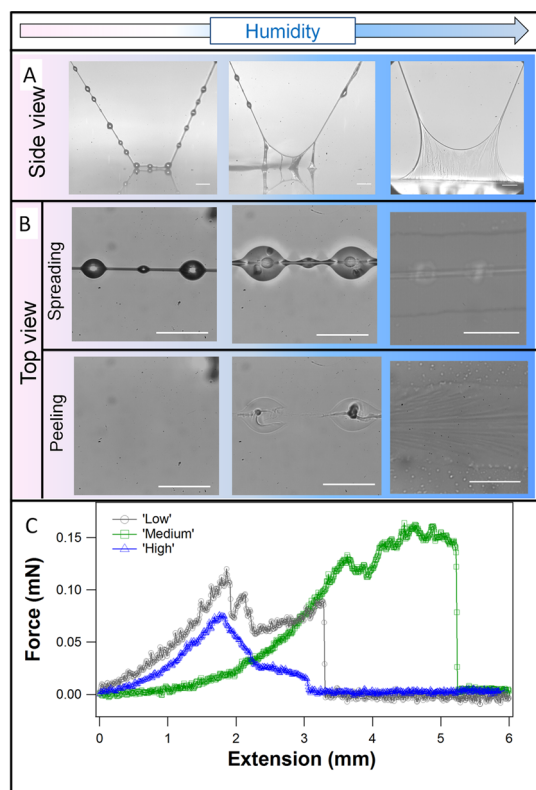


Figure 1. Work done during peeling of capture thread from five spider species at four different humidities. Top to bottom panels include species from the humid to dry habitat, respectively. Notice that for each species, the maximum adhesion occurs at the humidity closest to the foraging humidity of that spider species. Table 1 includes the full description of spider species and their habitats. The adhesion data were offset on the y-axis to clearly represent the trend with humidity. The ratio of maximum to minimum adhesion for each species is denoted on the left of each curve. The adhesion test was done over a sample size of >14 silk threads from various webs and spiders, and the actual peeling work values are reported in Table S1. The rate of pull-off was kept constant at  $1 \text{ mm(s)}^{-1}$ . The error bars represent standard error.

design for maximizing adhesion. The increase in work done by the flagelliform fibers with increase in humidity is consistent with the tensile data reported by Vollrath et al.<sup>11</sup> and shows that the water absorbed by hygroscopic salts plasticize both the fiber and the glue droplets.

Figure 2A,B shows the light microscope images of the *Larinioides* viscid silk thread during peeling at three humidity conditions, and the corresponding force–extension data are shown in Figure 2C. Figure 2A shows the side-view of glue droplets during peeling. At low humidity, the glue droplets do not spread much on the surface and remain intact during the peeling process. At high humidity, the droplets spread completely such that they coalesce to form a sheet of glue during peeling. The force profile of capture thread at high humidity shows a gradual decrease in force, suggesting that the sheet of glue thins into capillary bridge before breaking. At optimum humidity, the glue not only spreads to make contact on the surface but also strongly resists peeling. The peeling work is highest because both peak-force and extension are maximized. The force-strain profile of whole thread is



**Figure 2.** *Larinioides* captures thread peeling at  $0.1 \text{ mm}(\text{s})^{-1}$  in low, medium, and high humidity environment. (A) Side-view of capture thread peeling. Notice the increase in glue extensibility with humidity. (B) Top view shows the spreading and just before peeling images. Notice that at low humidity, the glue is completely peeled from the surface, but at high humidity, glue is left behind at the contact interface after peeling. At intermediate humidity, the glue peeled from the surface following a combination of interfacial and cohesive failure. (C) Typical force–extension graphs obtained for capture thread peeling at different humidities. The maximum peak-force and glue extension are achieved at optimum humidity, thereby maximizing the work (area under the curve) at medium humidity for *Larinioides* species. Scale bars are  $50 \mu\text{m}$ .

similar to the single glue droplet pull-off experiments as a function of humidity.<sup>6,27</sup>

Figure 2B demonstrates the top view during peeling, where we observe a transition from interfacial failure to cohesive failure as humidity increases. At low humidity, the glue is visually peeled off from the surface. But at high humidity, the glue was left behind at the contacting area. The reduction in viscosity makes the bulk strength significantly weaker than the interface, such that at high humidity, the glue fails cohesively. This trend was observed for all the spider species except *Tetragnatha*. For *Tetragnatha*, the glue viscosity did not reduce enough to observe cohesive failure even up to 90% RH. As seen in Figure 1, the *Tetragnatha* glue's peeling work kept increasing at humidities close to 100% RH.

**Maximizing Peeling Work.** Glue has to balance two antagonistic functions for adhesion: spreading to increase contact area and resisting peeling to dissipate

energy. That is, the peeling work is fundamentally a product of two factors: interfacial adhesion and bulk dissipation. The interfacial adhesion depends on interfacial bonds, which are related to the spreading area of the glue droplet and the strength of intermolecular interaction. The bulk dissipation depends on the viscosity/viscoelasticity of the glue droplet. The glue droplet absorbs moisture from the atmosphere with an increase in humidity<sup>6–9</sup> such that the glue becomes more fluid and extensible (Figure 2A). The spreading area depends on the initial volume of the drop and the rate of spreading. Both the glue spreading with time and the bulk dissipation are related to glue viscosity. Similar to a model used for viscoelastic adhesives (eq 1),<sup>22</sup> the total peeling work,  $U_T$  (J), is a product of interfacial adhesion energy,  $(W_a * A_{\text{glue}})$ , and bulk dissipation factor,  $f(V, T, \eta)$ .  $W_a$  ( $\text{J}/\text{m}^2$ ) is substrate–glue interaction energy, and  $A_{\text{glue}}$  ( $\text{m}^2$ ) is spreading area of glue, and  $f(V, T, \eta)$  is a function of rate of peeling ( $V$ ), temperature ( $T$ ), and viscosity ( $\eta$ ).  $T$  and  $\eta$  are dependent variables, as an increase in  $T$  generally reduces  $\eta$  of polymeric adhesives.<sup>28</sup> It is important to note that  $U_T$  is a product of two factors, and maximum adhesion is achieved when both contact area and bulk dissipation are optimized.

$$U_T = (W_a * A_{\text{glue}})(1 + f(V, T, \eta)) \quad (1)$$

In these experiments we kept thread peeling rate, thread contact time, and temperature constant. The parameters controlling the peeling work are viscosity, spreading area, and intermolecular interactions. To quantify the changes in viscosity and spreading area, we measure the spreading kinetics of the glue droplets as a function of RH using a high-speed camera and the experimental geometry shown in Figure 3A. The glue droplet is brought in contact with clean glass substrate, and the spreading of glue is observed on the glass substrate under transmitted light (see Experimental Section). Figure 3B shows time-lapse images of *Larinioides* glue spreading at different humidities. The glue droplets spread further and faster as the humidity increases. Notice that the initial size of droplet at  $t = 0$  doubles as the humidity increased from 30% to 90% RH due to the hygroscopic nature of the glue.<sup>6–8</sup>

**Measuring Glue Viscosity.** We normalize the glue spreading radius,  $r$ , on the substrate with the initial radius of the glue droplet,  $R$ . This helps to compare glue spreading kinetics at different humidities within and between species. To determine the range of viscosity for optimum adhesion, we quantify the spreading of liquid droplets on solid substrate using the following power law (eq 2)<sup>29,30</sup> which relates the spreading of a liquid droplet with the viscosity of the fluid:

$$\frac{r}{R} = \left(\frac{\gamma t}{\eta R}\right)^\beta \quad (2)$$

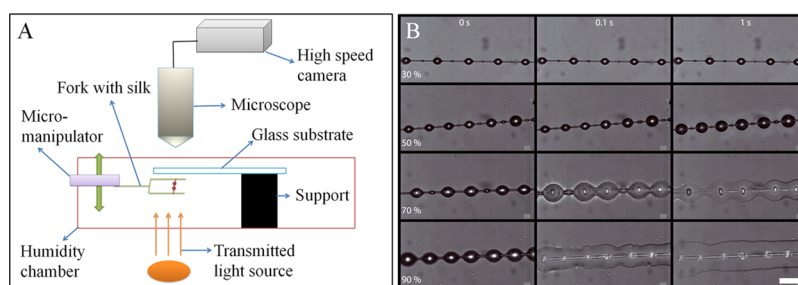


**Figure 3.** (A) Experimental setup to measure spreading of spider glue droplets under controlled humidity. (B) Time-lapse images of *Larinioides* spider glue droplets spreading under four different humidities. Notice that both rate and total glue spreading area increase with humidity. The differences in droplet sizes at  $t = 0$  s are due to the swelling of droplets during acclimation at higher humidities. Scale bar is  $50 \mu\text{m}$ .

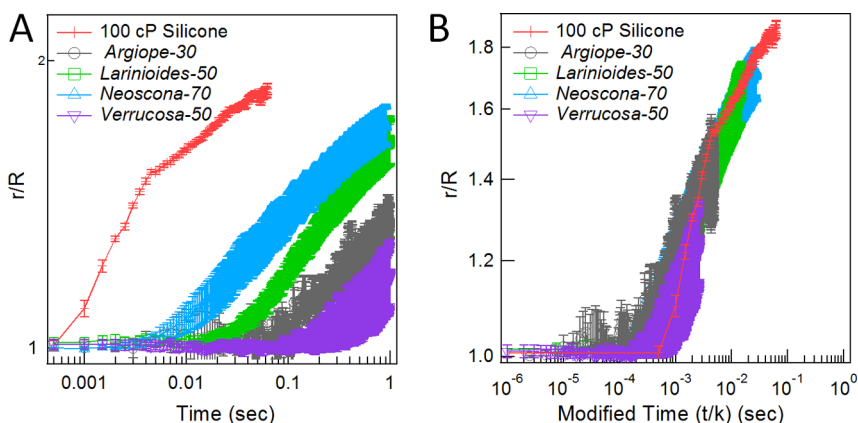


**Figure 4.** (A) Plot of normalized spreading radius ( $r/R$ ) vs time ( $t$ ) for four spider species at the humidity of maximum adhesion and  $\sim 100$  cP Silicone polymer. (B) Normalized spreading radius ( $r/R$ ) plotted with a modified time axis ( $t/k$ ), where  $k$  is the shift-factor required to overlap the spreading graphs on a master curve (see SI-6). Please note that spreading beyond the initial droplet radius was not visible until  $\sim 0.01$  s (see text). The sample size used for these measurements is provided in Table S3.

where  $r$  is radius of the spreading front on the substrate,  $R$  is the initial radius of the liquid droplet,  $\gamma$  is surface tension,  $\eta$  is viscosity,  $t$  is time, and  $\beta$  is a constant that depends on the time interval during spreading.<sup>29</sup> Since this law has been tested for liquid droplets but not for liquid droplets on a thread, we first constructed model glue droplets consisting of silicone polymer of different viscosities as beads on a nylon thread.<sup>14</sup> We measured ( $r/R$ ) as a function of time and used the concept of shift-factor to calculate the change in viscosity with respect to a reference polymer viscosity, which in this case was  $\sim 100$  cP. The use of the shift-factor does not depend on the validity of the power law, but only on the dimensionless parameter, ( $\gamma t/\eta R$ ). The expected and calculated viscosity values were within a factor of 2 of each other (SI-5), validating the procedure for analyzing the changes in viscosity as a function of humidity in spider glue.

We further use the shift-factor concept to calculate the glue viscosity as a function of humidity. Figure 4A shows the glue spreading with time at the humidity of maximum adhesion for four spider species. As a comparison we include the spreading for  $\sim 100$  cP silicone liquid. We rescale the x-axis using shift-factor to overlap all the data in Figure 4A on a master curve (Figure 4B). The shift-factors are then used to calculate

the viscosity using the eq 2 (SI-6). Table 2 shows the glue viscosity range for four spider species and the viscosity at humidity of maximum adhesion condition. The results show that there exists a narrow range of viscosity value where adhesion is maximized. The viscosity of glue in four spider species changes over 5 orders of magnitude, but maximum adhesion is achieved in a narrow range of viscosity,  $10^5$ – $10^6$  cP, even though viscosity is achieved at very different humidities for each species.

*Tetragnatha* glue viscosity is not calculated because of the small size of the glue droplets ( $\sim 10 \mu\text{m}$  diameter), which resulted in interference fringes<sup>31</sup> around the droplet boundary, thereby making it difficult to track the spreading front (Figure S10). However, a number of qualitative observations suggest that *Tetragnatha* glue is more viscous than the glue of other four species. Unlike other species, *Tetragnatha* glue was not observed to spread beyond the initial radius for  $t < 1$  s at 50% RH (SI-6). At 90% RH, the *Tetragnatha* glue spread to a maximum size of  $\sim 1.5\times$  the original size, while the glue droplets of other four species spread to almost twice the initial radius (Figure S2). Furthermore, upon peeling at 90% RH, we observe a mixture of interfacial and cohesive failure for *Tetragnatha* glue, while other species at high humidity

**TABLE 2. Viscosity of Spider Glue from Diverse Spider Species Measured at the Humidity of Maximum Adhesion<sup>a</sup>**

species	humidity at maximum		
	adhesion (% RH)	viscosity (cP)	viscosity range (cP)
<i>Argiope</i>	30	$\sim 7 \times 10^5$	$10^3$ – $10^6$
<i>Larinioides</i>	50	$\sim 1 \times 10^5$	$10^3$ – $10^8$
<i>Verrucosa</i>	50	$\sim 8 \times 10^5$	$10^3$ – $10^7$
<i>Neoscona</i>	70	$\sim 6 \times 10^4$	$10^3$ – $10^8$
<i>Tetragnatha</i>	90	—	—

<sup>a</sup> Notice that the glue viscosity varies over five orders of magnitude with humidity, yet the maximum adhesion is achieved in narrow range of viscosity,  $10^5$ – $10^6$  cP. *Tetragnatha* viscosity could not be calculated because of its small-sized glue droplets and interference fringes formation around the droplet boundary (see text and Figure S10).

show significant cohesive failure such that all the glue is left behind at the contact interface (Figure 2B). These observations suggest that the viscosity of *Tetragnatha* glue viscosity is higher than the optimal viscosity required for adhesion and that this range was not reached even until 90% RH.

## DISCUSSION

Figure 5 depicts the principle behind spider glue's humidity responsive adhesion. From eq 1, the total peeling work is a product of two terms: surface interaction and bulk dissipation. The surface interaction term, ( $W_a * A_{glue}$ ), is a product of substrate–glue interaction energy and the spreading area. We do not expect the substrate–glue interaction energy to be a function of humidity, but the spreading area increases significantly with humidity. Figure 5A shows spreading area for *Larinioides* plotted after 1 s of contact time. The choice of 1 s contact time is both ecologically relevant<sup>32</sup> and similar to adhesion test conditions (Figure 1). The bulk dissipation term, ( $f(V, \eta)$ ), is a function of rate of peeling and viscosity. Here we kept the peeling rate constant, and the viscosity decreases sharply with an increase in humidity (Figure 5A, *Larinioides*). Single glue droplet adhesion measurements for *Larinioides* show that the viscous dissipation energy decreases sharply with an increase in humidity.<sup>6</sup> Because the total peeling work is a product of surface interaction and bulk dissipation and both these factors vary with a opposite trend with a change in humidity, we expect that the adhesion will be maximized at an intermediate humidity (Figure 5B). We find that this optimum humidity is specific to each species and is preferred for its foraging habitat. Thus, adaptation of spider glue to a particular microhabitat could easily occur through shifts in how glue viscosity responds to humidity.

## CONCLUSION

Many biological systems modulate viscosity for a variety of functions. Bacteria cytoplasm turns glassy

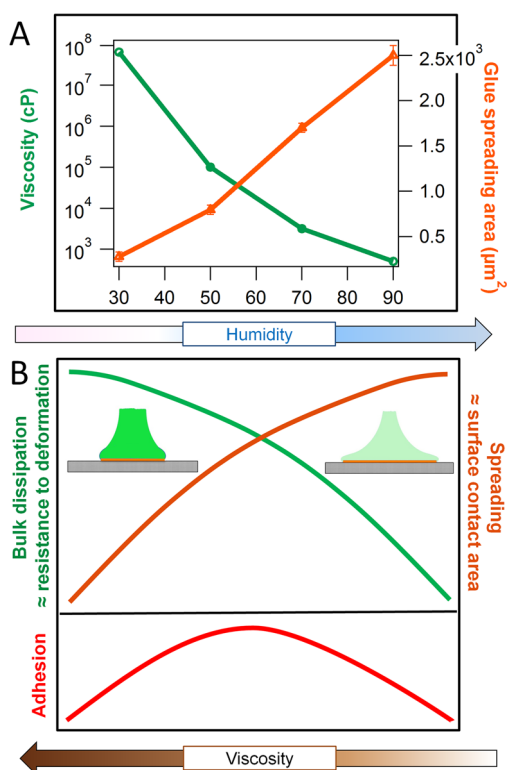


**Figure 5. Model for spider glue's humidity responsive adhesion. (A)** The measured viscosity (cP) and glue droplet spreading area (after 1 s of contact time)<sup>32</sup> is plotted against humidity for *Larinioides* spider species. The spreading area was measured from top-view (Figure 2B), except for 30% RH, where the area was measured from side-view as the droplets did not spread beyond their initial size in 1 s contact time (see Experimental Section). **(B)** As the humidity increases, the glue viscosity decreases significantly. A decrease in glue viscosity increases the spreading area but reduces the bulk dissipation. Since adhesion is a product of spreading area and bulk-dissipation (eq 1), there exists an optimum humidity wherein adhesion is maximized. Spider species tune glue viscosity to maximize capture thread adhesion at different humidities.

during dormancy to reduce metabolic activity.<sup>33</sup> Flies use low-viscosity secretions to enable quick detachment,<sup>34</sup> chameleons<sup>35</sup> use highly viscous secretions to catch prey, and velvet worms<sup>36</sup> and spitting spiders<sup>37</sup> subdue prey by entangling them in quick-hardening glues. But spider species are exceptional in how their glue viscosity is tuned to perform optimally at the foraging humidity of their natural habitat. For spider glue, the capillary forces are much smaller in comparison to the viscous/viscoelastic forces,<sup>27,38,39</sup> and tuning of glue viscosity is an efficient way of maximizing adhesion for prey capture.

So, how do spider species tune their glue viscosity? The known glycoproteins in spider glues show  $\sim 10\%$  variation in sequence across spider species,<sup>16</sup> but the salt composition is highly variable.<sup>17,18,40</sup> Since hygroscopic salts determine the humidity responsiveness of the spider glue by absorbing water and providing protein mobility,<sup>20</sup> these protein-salt combinations appear to have been the target of natural

selection that contributes to the nonlinear response of bulk glue viscosity to humidity. Investigating the role of individual salt components on protein mobility and bulk viscoelasticity would help in understanding how salts tune the glue viscosity, and

ultimately the glue adhesion. The addition of low molecular weight organic salts to hygroscopic adhesives can therefore provide a mechanism to tune the performance of the next generation of synthetic adhesives.

## EXPERIMENTAL SECTION

**Spider Care and Sample Collection.** Naturally spun orb webs of *Neoscona* and *Verrucosa* were collected near Blacksburg, VA, USA. *Larinioides*, *Argiope*, and *Tetragnatha* were collected in Akron, OH, USA. All the spiders were housed in separate cages and fed a weekly diet of crickets. Silk samples were collected onto cardboard mounts with a 5 mm inch hole in the center. Only regions directly below the spiders hub were collected in order to remain consistent and limit within web variation. The procured orb webs were stored in laboratory environment at  $22 \pm 2$  °C and  $30 \pm 5\%$  RH and tested within 2 weeks of collection. No significant difference was observed in the adhesion of fresh and 2 week-aged samples.<sup>41</sup>

**Adhesion Testing.** Individual threads of capture spiral silk were collected from the webs and adhered to rectangular cardboard mounts across 12.58 mm gaps. We used an MTS Nano Bionix for adhesion measurements. The samples were equilibrated at the desired humidity for 3 min and brought in contact with a 5 mm wide piece of glass mounted on a small clamp. The sample was first lowered until it initially contacted the glass and then pressed down until the force registered 50 mN, to ensure firm contact. The sample was kept in contact for 6 s before pulling away from the substrate at a constant rate of  $0.1 \text{ mm(s)}^{-1}$ . The area under the load–displacement curve represents the energy required to separate the thread from the glass substrate (referred to as peeling work). The glass substrates were cleaned by washing them with isopropyl alcohol and deionized water. After every test, we advanced the new thread 0.125 mm to ensure that every run was performed on a clean glass surface. The sample size for the number of capture threads tested for each species under each humidity is compiled in Table S2.

**Glue Droplet Spreading.** We used an Olympus BX53 microscope with 20 $\times$ , 50 $\times$ , and 100 $\times$  objectives. A custom-built humidity chamber controlled the ambient humidity around the droplet. A clean hydrophilic glass substrate was placed between the microscope and the droplet, and the silk thread with glue droplets was brought in contact with the substrate. This motion is referred to as immobilization of the glue droplet. The entire process was observed under transmitted light. Due to the spherical shape of the droplet, a bright spot of light was observed on the topmost point of the droplet. At the time of immobilization, there was a distinct change in the intensity of this spot, which was considered as  $t = 0$  (SI-7). We used a Photron FASTCAM SA3 camera to observe the glue droplet immobilization process at 1000–2000 frames per second (fps). Transmitted light ensured contrast and resolution for accurate tracking of the droplet boundary at 50 $\times$  and 100 $\times$  magnification. However, in this geometry, the spreading front could be tracked only after it had spread beyond the original radius of the droplet. The spreading front was therefore not tracked between the time the drop made the initial contact to the time the spreading front reached the size of the initial radius of suspended droplet.

The silk thread was equilibrated at a particular humidity before the immobilization. The humidity and the volume of the glue droplet are constant during immobilization. The silk glue droplet increases its volume by absorbing water from the atmosphere at higher humidities. A motor controlled manipulator brought the natural spider silk thread into contact with the substrate at a velocity of  $0.1 \text{ mm(s)}^{-1}$ , a value significantly less than the early spreading velocity of glue. The size of the glue droplet varied across the species,<sup>8</sup> but all were significantly smaller than the possible capillary length of the droplets (SI-8). The transparent glass substrates were cleaned by sonicating for

15 min each in chloroform and acetone, followed by drying in  $\text{N}_2$  gas. The sample size for the number of glue droplets tested for each species under each humidity is compiled in Table S3. Videos were captured at 2000 fps, with the exception of *Tetragnatha* and the synthetic polymer droplets, which were filmed at 1000/500 fps. The droplet size was tracked on each frame of the video, which varied in length from 800 to 5000 frames. From the side view, we observed complete wetting of glue on the glass substrate under all humidities measured (Figure 2A).

**Video Analysis.** Videos were analyzed using ProAnalyst motion analysis software (XCiteX, Inc., Cambridge, MA, USA). Between one and six droplets were chosen from each video depending on the size of the glue droplets and the optical magnification used. Individual coordinate systems were created for each droplet, originating at their respective centers. The axial direction along the fiber was chosen as the  $x$ -axis, and the radius was tracked on the orthogonal  $y$ -axis direction. The spreading front was tracked only after it had spread beyond the original dimension of the droplet. The initial contact was immediately noticeable by a characteristic color change as light began to refract through the substrate–droplet layer (SI-7). The measured coordinates were then translated into droplet radius values.

**Viscosity Calculations.** Surface tension of glue was determined by measuring surface tension of model aqueous salt solutions of similar concentration of salts as found in *Larinioides* species (SI-4). Even though we do not know the absolute value of surface tension of spider glue, the range of possible surface tension values are  $\sim 30$ – $70 \text{ mN/m}$ , which is significantly less than the orders of magnitude variation in the viscosity of the glue (Figure 4A and SI). Hence, we have used an average measured value of surface tension ( $65 \text{ mN/m}$ ) for calculating the approximate glue viscosity. Also, an increase in humidity may condense water on glass resulting in a change in effective surface energy of substrate. However, the effect of change in substrate wettability on the spreading power law is only observed in the late stages of spreading ( $t \sim 1 \text{ s}$ ),<sup>29,30</sup> and its effect is expected to be much smaller than the actual changes in glue viscosity as a function of humidity.

**Conflict of Interest:** The authors declare no competing financial interest.

**Acknowledgment.** We thank Jack Gillespie and Edward Laughlin for their help with the fabrication of silk thread mounts and Dr. Mark A. Townley for providing the synthetic salt samples. We acknowledge support from National Science Foundation grant IOS-1257719.

**Supporting Information Available:** The Supporting Information is available free of charge on the ACS Publications website at DOI: 10.1021/acsnano.5b05658.

Details of adhesion tests, use of shift-factor in determining viscosity from glue droplet spreading experiments, effect of salt concentration on surface tension of water, and calculations of capillary length (PDF)  
Immobilization of *Verrucosa* spider capture thread on a glass substrate at 50% RH. (AVI)

## REFERENCES AND NOTES

1. Elbaum, R.; Zaltzman, L.; Burgert, I.; Fratzl, P. The Role of Wheat Awns in the Seed Dispersal Unit. *Science* **2007**, *316*, 884–886.
2. Fratzl, P.; Barth, F. G. Biomaterial Systems for Mechano-sensing and Actuation. *Nature* **2009**, *462*, 442–448.

3. Lin, H.; Lizarraga, L.; Bottomley, L. A.; Meredith, J. C. Effect of Water Absorption on Pollen Adhesion. *J. Colloid Interface Sci.* **2015**, *442*, 133–139.
4. Tan, K. T.; Vogt, B. D.; White, C. C.; Steffens, K. L.; Goldman, J.; Satija, S. K.; Clerici, C.; Hunston, D. L. On the Origins of Sudden Adhesion Loss at a Critical Relative Humidity: Examination of Bulk and Interfacial Contributions. *Langmuir* **2008**, *24*, 9189–9193.
5. White, C.; Tan, K. T.; Hunston, D.; Steffens, K.; Stanley, D. L.; Satija, S. K.; Akgun, B.; Vogt, B. D. Mechanisms of Criticality in Environmental Adhesion Loss. *Soft Matter* **2015**, *11*, 3994–4001.
6. Sahni, V.; Blackledge, T. A.; Dhinojwala, A. Changes in the Adhesive Properties of Spider Aggregate Glue During the Evolution of Cobwebs. *Sci. Rep.* **2011**, *1*, 41.
7. Opell, B. D.; Karinshak, S. E.; Sigler, M. A. Humidity Affects the Extensibility of an Orb-Weaving Spider's Viscous Thread Droplets. *J. Exp. Biol.* **2011**, *214*, 2988–2993.
8. Opell, B. D.; Karinshak, S. E.; Sigler, M. A. Environmental Response and Adaptation of Glycoprotein Glue Within the Droplets of Viscous Prey Capture Threads from Araneoid Spider Orb-Webs. *J. Exp. Biol.* **2013**, *216*, 3023–3034.
9. Stellwagen, S. D.; Opell, B. D.; Short, K. G. Temperature Mediates the Effect of Humidity on the Viscoelasticity of Glycoprotein Glue Within the Droplets of an Orb-Weaving Spider's Prey Capture Threads. *J. Exp. Biol.* **2014**, *217*, 1563–1569.
10. *World Spider Catalog, 2015*; <http://wsc.nmbe.ch> (accessed January 26, 2015).
11. Vollrath, F.; Edmonds, D. T. Modulation of the Mechanical Properties of Spider Silk by Coating with Water. *Nature* **1989**, *340*, 305–307.
12. Blackledge, T. A.; Scharff, N.; Coddington, J. A.; Szuüts, T.; Wenzel, J. W.; Hayashi, C. Y.; Agnarsson, I. Reconstructing Web Evolution and Spider Diversification in the Molecular Era. *Proc. Natl. Acad. Sci. U. S. A.* **2009**, *106*, 5229–5234.
13. Vollrath, F.; Tillinghast, E. Glycoprotein Glue Beneath a Spider Web's Aqueous Coat. *Naturwissenschaften* **1991**, *78*, 557–559.
14. Sahni, V.; Labhasetwar, D.; Dhinojwala, A. Spider Silk Inspired Functional Microthreads. *Langmuir* **2012**, *28*, 2206–2210.
15. Vollrath, F.; Fairbrother, W. J.; Williams, R. J. P.; Tillinghast, E. K.; Bernstein, D. T.; Gallagher, K. S.; Townley, M. A. Compounds in the Droplets of the Orb Spider's Viscid Spiral. *Nature* **1990**, *345*, 526–528.
16. Chores, O.; Bayarmagnai, B.; Lewis, R. V. Spider Web Glue: Two Proteins Expressed from Opposite Strands of the Same DNA Sequence. *Biomacromolecules* **2009**, *10*, 2852–2856.
17. Townley, M. A.; Bernstein, D. T.; Gallagher, K. S.; Tillinghast, E. K. Comparative Study of Orb Web Hygroscopicity and Adhesive Spiral Composition in Three Araneid Spiders. *J. Exp. Zool.* **1991**, *259*, 154–165.
18. Townley, M. A.; Tillinghast, E. K. In *Spider Ecophysiology*; Nentwig, W., Ed.; Springer-Verlag: Berlin, 2013; Chapter Aggregate Silk Gland Secretions of Araneoid Spiders, pp 283–302.
19. Amarpuri, G.; Chaurasia, V.; Jain, D.; Blackledge, T. A.; Dhinojwala, A. Ubiquitous Distribution of Salts and Proteins in Spider Glue Enhances Spider Silk Adhesion. *Sci. Rep.* **2015**, *5*, 9030.
20. Sahni, V.; Miyoshi, T.; Chen, K.; Jain, D.; Blamires, S. J.; Blackledge, T. A.; Dhinojwala, A. Direct Solvation of Glycoproteins by Salts in Spider Silk Glues Enhances Adhesion and Helps To Explain the Evolution of Modern Spider Orb Webs. *Biomacromolecules* **2014**, *15*, 1225–1232.
21. Opell, B.; Hendricks, M. The Role of Granules Within Viscous Capture Threads of Orb-Weaving Spiders. *J. Exp. Biol.* **2010**, *213*, 339–346.
22. Gent, A. Adhesion and Strength of Viscoelastic Solids. Is There a Relationship Between Adhesion and Bulk Properties? *Langmuir* **1996**, *12*, 4492–4496.
23. Mcnett, B. J.; Rypstra, A. L. Habitat Selection in a Large Orb-Weaving Spider: Vegetational Complexity Determines Site Selection and Distribution. *Ecol. Entomol.* **2000**, *25*, 423–432.
24. Cera, I.; Spunđis, V.; Meleci, V. Occurrence of Grass-Dwelling Spiders in Habitats of Lake Engure Nature Park. *Environ. Exp. Biol.* **2010**, *8*, 59–69.
25. Bradley, R. *Common Spiders of North America*; University of California Press: Berkeley, CA, 2013.
26. Adams, M. Choosing Hunting Sites: Web Site Preferences of the Orb Weaver Spider, *Neoscona crucifera*, Relative to Light Cues. *J. Insect Behav.* **2000**, *13*, 299–305.
27. Sahni, V.; Blackledge, T.; Dhinojwala, A. Viscoelastic Solids Explain Spider Web Stickiness. *Nat. Commun.* **2010**, *1*, 19.
28. Gent, A.; Petrich, R. Adhesion of Viscoelastic Materials to Rigid Substrates. *Proc. R. Soc. London, Ser. A* **1969**, *310*, 433–448.
29. Eddi, A.; Winkels, K. G.; Snoeijer, J. H. Short Time Dynamics of Viscous Drop Spreading. *Phys. Fluids* **2013**, *25*, 013102.
30. Chen, L.; Bonaccorso, E. Effects of Surface Wettability and Liquid Viscosity on the Dynamic Wetting of Individual Drops. *Phys. Rev. E* **2014**, *90*, 022401.
31. Heinrich, V.; Wong, W. P.; Halvorsen, K.; Evans, E. Imaging Biomolecular Interactions by Fast Three-Dimensional Tracking of Laser-Confined Carrier Particles. *Langmuir* **2008**, *24*, 1194–1203.
32. Blackledge, T. A.; Zevenbergen, J. M. Mesh Width Influences Prey Retention in Spider Orb Webs. *Ethology* **2006**, *112*, 1194–1201.
33. Parry, B. R.; Surovtsev, I. V.; Cabeen, M. T.; O'Hern, C. S.; Dufresne, E. R.; Jacobs-Wagner, C. The Bacterial Cytoplasm has Glass-like Properties and is Fluidized by Metabolic Activity. *Cell* **2014**, *156*, 183–194.
34. Peisker, H.; Heepe, L.; Kovalev, A. E.; Gorb, S. N. Comparative Study of the Fluid Viscosity in Tarsal Hairy Attachment Systems of Flies and Beetles. *J. R. Soc., Interface* **2014**, *11*, 20140752.
35. Brau, F.; Lanterbecq, D.; Zghikh, L.-N.; Bels, V.; Damman, P. Is Viscous Adhesion Strong Enough to Allow Prey Capture by Chameleons? [arXiv:physics/14116126v1](http://arxiv.org/abs/1411.6126v1). <http://arxiv.org/abs/1411.6126v1>, **2014**.
36. Concha, A.; Mellado, P.; Morera-Brenes, B.; Costa, C. S.; Mahadevan, L.; Monge-Nájera, J. Oscillation of the Velvet Worm Slime Jet by Passive Hydrodynamic Instability. *Nat. Commun.* **2015**, *6*, 6292.
37. Suter, R. B.; Stratton, G. E. In *Spider Ecophysiology*; Nentwig, W., Ed.; Springer-Verlag: Berlin, 2013; Chapter Predation by Spitting Spiders: Elaborate Venom Gland, Intricate Delivery System, pp 241–251.
38. Cheung, E.; Sitti, M. Adhesion of Biologically Inspired Oil-Coated Polymer Micropillars. *J. Adhes. Sci. Technol.* **2008**, *22*, 569–589.
39. Cheung, E.; Sitti, M. Enhancing Adhesion of Biologically Inspired Polymer Microfibers with a Viscous Oil Coating. *J. Adhes.* **2011**, *87*, 547–557.
40. Townley, M. A.; Tillinghast, E. K.; Neefus, C. D. Changes in Composition of Spider Orb Web Sticky Droplets with Starvation and Web Removal, and Synthesis of Sticky Droplet Compounds. *J. Exp. Biol.* **2006**, *209*, 1463–1486.
41. Opell, B. D.; Schwend, H. S. Persistent Stickiness of Viscous Capture Threads Produced by Araneoid Orb-Weaving Spiders. *J. Exp. Zool., Part A* **2008**, *309*, 11–16.